

The Generation of Growth Dislocations by Inclusions and Growth-Face Damages: An Experimental Study

Gero Neuroth and Helmut Klapper*

The generation of growth dislocations in crystals by intentionally introduced foreign-particle inclusions and by mechanical damaging (scratching) of the growth face is reported. The formation of dislocations is studied by in situ observation of the step pattern on the involved growth face by optical microscopy and—after growth—by X-ray diffraction topography. This is performed on three different growth faces of orthorhombic salol ($C_{13}H_{10}O_3$, melting temperature $T_m = 41.5^\circ\text{C}$) growing from the melt supercooled by $1\text{--}2^\circ\text{C}$. The development of the growth pattern after the closure of the inclusion by overgrowing layers and after the scratching is recorded by videos. Particularly instructive is the inclusion experiment on the fast-growing (100) face: immediately after the closure a big pyramid and fast step source appears, which dominates and sporadically overflows neighbored secondary step sources. In the sequel the big pyramid splits into a row of small hills which gradually diverge. This indicates that the associated dislocations fan out within the (010) plane of the crystal, as is confirmed by X-ray topography. The in situ scratching of the growth face triggers the immediate appearance and fast development of a complex hill structure associated with numerous dislocations.

play a key role in the formation of growth dislocations. These are dislocations connected to the growth front, with which they propagate during growth. They result from “lattice closure errors” which arise when an inclusion is “closed” by overgrowing layers. These layers meet with local offsets which provide the Burgers vectors of the dislocations initiated by them. Since these dislocations propagate with directions roughly perpendicular to the growth front, the crystal region “behind” the inclusions (viewed in growth direction) usually contains growth dislocations.^[1,2] In a similar fashion, growth dislocations originate from all kinds of defects of the growth face.

In contrast to *primary* inclusions, *secondary* inclusions are precipitates of solute impurities (dopants) formed after growth during cooling, annealing, or processing of the crystals. They are not connected to the growth front and do not lead to growth dislocations. They frequently

are the source of glide dislocations in the shape of loops or half-loops, which result from the relaxation of stress (post-growth dislocations^[1,2]). Secondary inclusions are not discussed here.

We report on the generation of growth dislocations by intentionally introduced foreign-particle inclusions and by mechanical damaging (scratching) of the growth face.^[3,4] The formation of dislocations is studied by in situ observation of the step pattern on the involved growth face and—after growth—by X-ray diffraction topography. This was performed on three different growth faces of orthorhombic salol ($C_{13}H_{10}O_3$), melting temperature ($T_m = 41.5^\circ\text{C}$) growing from the melt supercooled by $1\text{--}2^\circ\text{C}$.^[5] Salol is a very suitable model crystal for this kind of experiments because of its convenient melting temperature T_m , its stability against secondary nucleation even at high supercooling, and the relatively high growth rates (up to 1 mm h^{-1}) compared with crystals growing from solutions. Accordingly, the velocities of the defect formation and the associated processes on the growth face are so high that an experiment can be conducted within a few hours only. **Figure 1** shows the typical shape of a salol crystal grown at supercooling of about 2°C . The inclusion and scratching experiments have been performed on faces showing different growth rates: (100) (fast), (111) (medium), and (010) (slow).

Organic melts contain a considerable amount of dissolved atmospheric gas which is absorbed when the starting material is

1. Introduction

All kinds of *primary* inclusions (foreign particles, solvent inclusions, gas bubbles) incorporated into the crystals during growth

Dr. G. Neuroth^[+], Prof. H. Klapper
Steinmann Institut
(Mineralogisch-Petrologisches Institut)
University of Bonn
D-53113 Bonn Germany
Prof. H. Klapper
Institut für Kristallographie
RWTH Aachen University
D-52056 Aachen, Germany
E-mail: klapper@ifk.rwth-aachen.de

 The ORCID identification number(s) for the author(s) of this article can be found under <https://doi.org/10.1002/crat.201900159>

[+]Present address: Infineon Technologies GmbH & Co. KG, 01099 Dresden, Germany

© 2019 The Authors. Published by WILEY-VCH Verlag GmbH & Co. KGaA, Weinheim. This is an open access article under the terms of the Creative Commons Attribution-NonCommercial-NoDerivs License, which permits use and distribution in any medium, provided the original work is properly cited, the use is non-commercial and no modifications or adaptations are made.

DOI: 10.1002/crat.201900159

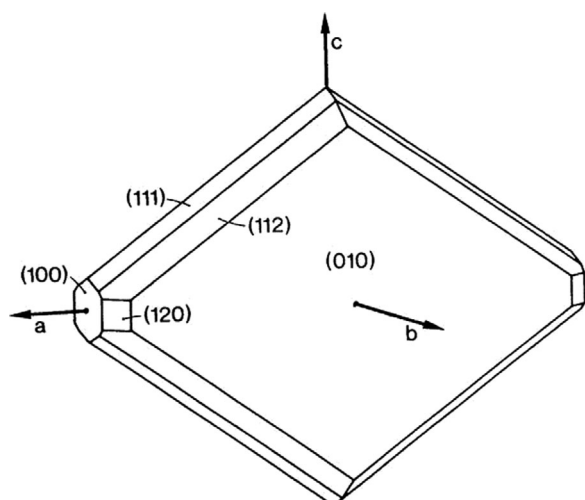


Figure 1. Typical morphology of salol $C_{13}H_{10}O_3$ (orthorhombic, $T_m = 41.5^\circ\text{C}$) grown from the melt supercooled by about 1.5°C .

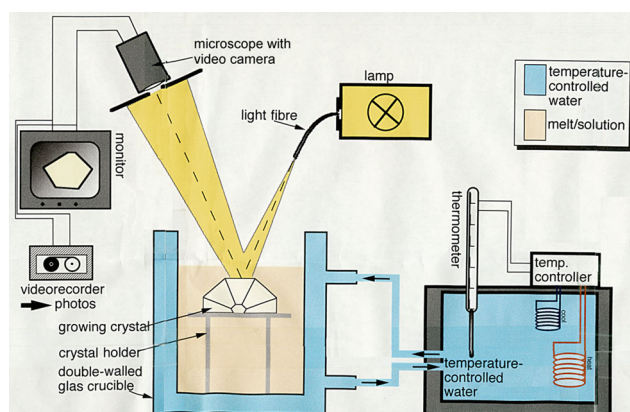


Figure 2. Illustration of the experimental setup for the in situ observation of the surface pattern of the growing crystal.

fused. Local increases of the growth rate may lead to the precipitation of gas and the formation of bubbles which in turn are the origins of growth dislocations. This has happened in a few cases of our inclusion and scratch experiments.

2. Experimental Section

The experimental setup is illustrated in **Figure 2**.^[3] The growth vessel is a hollow-walled glass container fed with temperature-controlled water adjusted to $1\text{--}2^\circ\text{C}$ below T_m . A seed crystal, cut from a previously grown crystal, was mounted on a small glass table in such a way that during growth the chosen habit face, (010), (100), or (111), was horizontally formed. When after $0.5\text{--}1\text{ h}$ the slowly growing face appeared to be visually flat and perfect, a solder ball (diameter $\approx 0.5\text{ mm}$) was dropped on this face, or the face was slightly scratched with a bent-open paper clip (diameter 0.5 mm). The development of the surface step pattern on this face was observed with a large-focal-distance microscope, including video records. The spatial and depth resolution was restricted, steps of heights $<10\text{ }\mu\text{m}$ were practically not visible.

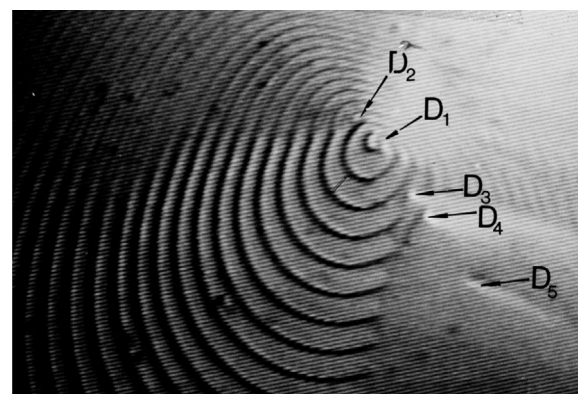


Figure 3. Surface pattern on a (111) growth face, 5 h after a short scratch. $D_1\text{--}D_5$ screw dislocations. D_1 emerges from the top of a pyramid and emits on one side (left) macrosteps of widths $0.02\text{--}0.05\text{ mm}$. On the other flank of the pyramid steps are not visible, probably due to the interaction with the step sources of the other dislocations. The region of unresolved steps extends with increasing influence of dislocations D_3 , D_4 . Width of image $\approx 2\text{ mm}$. (Video S1, Supporting Information).

After completion of the experiments a plate of $1\text{--}2\text{ mm}$ thickness was cut out of the crystal with a thread solution saw (solvent: xylene) in such a way that it contained the ball inclusion and the region “behind” the inclusion (viewed in growth direction). The slice was gently polished on a soft cloth soaked with xylene and the remains of the solvent squirted off with distilled water. The Lang-method of X-ray transmission topography^[6,7] with $\text{CuK}\alpha$ radiation and X-ray film Structurix D4 (Agfa) was used.

3. Results and Discussion

The essential features of the generation and subsequent development of dislocations after the ball inclusion and mechanical damage of the growth face are instructively disclosed by the video records, the playback of which are given in original velocity. The videos are accessible in the online version. Selected snapshots are given in **Figures 3–5**, **7**, **8** and **10** and explained in the figure captions. Video S1, Supporting Information (Figure 3) shows the interaction of the step sources of a dominating screw dislocation with several secondary screw dislocations above a small mechanical impact on a (111) face (medium growth rate), Video S2, Supporting Information (Figure 4) the slow development of a pyramid formed by macrosteps on a (010) face (low growth rate). **Figure 6** shows face (100) just before the ball inclusion is closed by overgrowing layers and illustrates the formation of a “wake” behind the ball in the direction of the step flow.

Videos S3, S4, and S5, Supporting Information (Figures 5, 7, 8) are particularly informative because they show in three selected sections the sometimes lively varying surface pattern of the fast-growing (100) face from dropping the metal ball until growth of about 8 mm above the inclusion. After this stage of growth new effects, exempt from a further fanning out of the dislocations, did not occur. In order to trace the further propagation of these dislocations by X-ray topography, the growth was continued until a crystal size of about 20 mm diameter. Topograph **Figure 9** shows these dislocations in full length from the inclusion to the final surface of the crystal. It also shows that the crystal grew

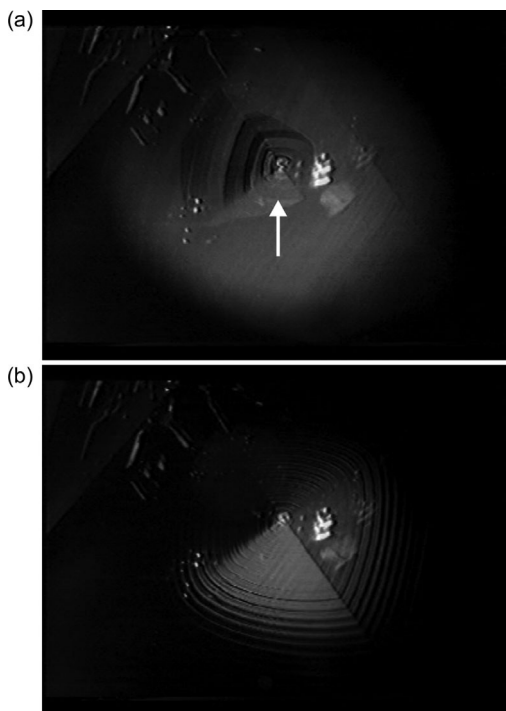


Figure 4. a) Growth pyramid formed above the ball inclusion (arrow) on the prominent (010) face (cf. Figure 1). b) The pyramid about 1 min later. The relative slow development of the pyramid is in accordance with the slow growth rate of this face. (Video S2, Supporting Information).

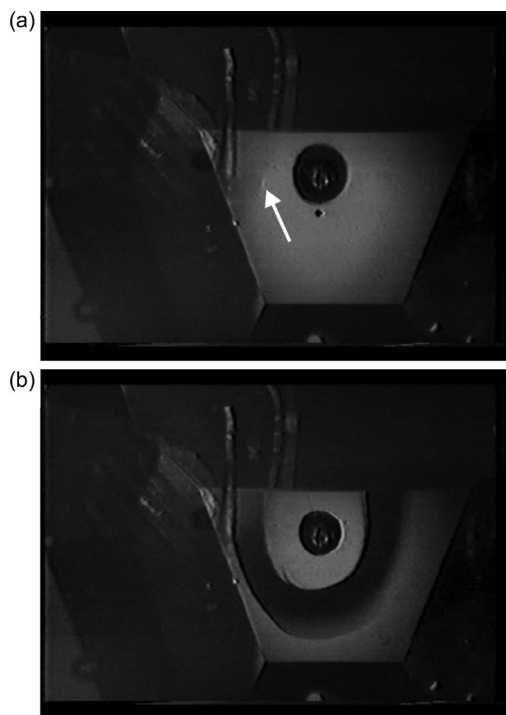


Figure 5. a) Solder ball (diameter ≈ 0.5 mm) just dropped on a (100) face free from visible growth steps. Arrow: a dislocation forming a flat hill. b) A huge macrostep of 0.5 mm width and about 0.1 mm height is spreading out from the ball. The "new" face is again free from visible steps. Width of snapshot ≈ 5 mm. (Video S3, Supporting Information).

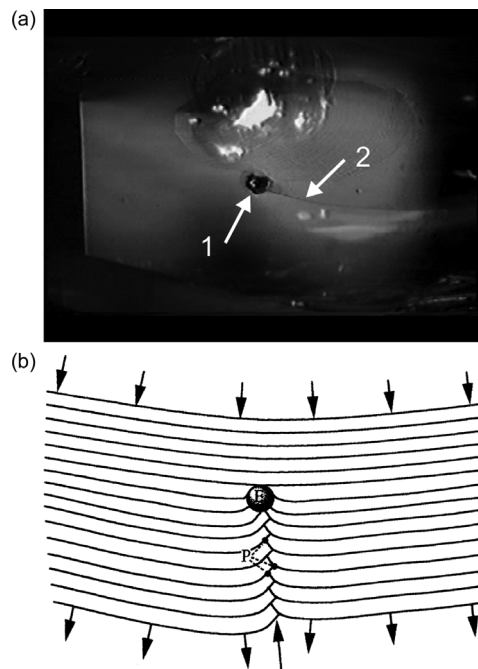


Figure 6. a) Continuation of Figure 5. The ball (arrow 1) is not yet covered by growth layers. The defect in the upper part of the figure is a gas inclusion precipitated from the melt. It also generates dislocations emitting growth steps. b) The formation of the "wake" [see arrow 2 in (a)] by interlacing of steps behind the ball in the direction of the step flow.

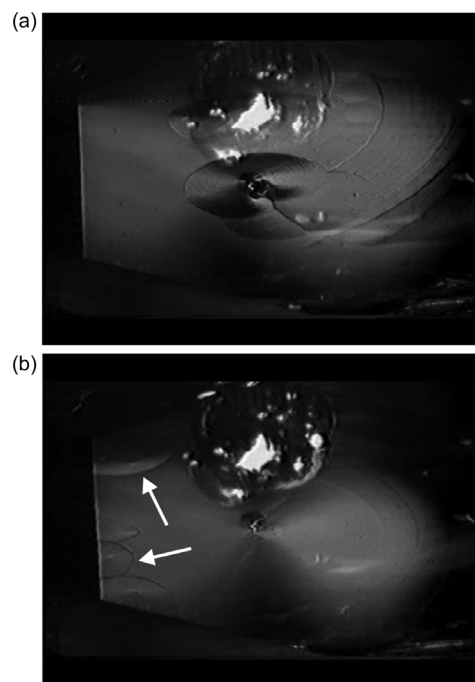


Figure 7. Continuation of Figure 5. a) The ball inclusion is just covered by growth layers. A sequence of fast concentric growth steps is emitted from the covering point, where a dominating growth hill is formed. In the following course secondary hills appear [arrows in (b)] and vanish again, submerged by the step flow of the dominant hill. (The record of this video is several times intentionally interrupted for a few minutes). (Video S4, Supporting Information).

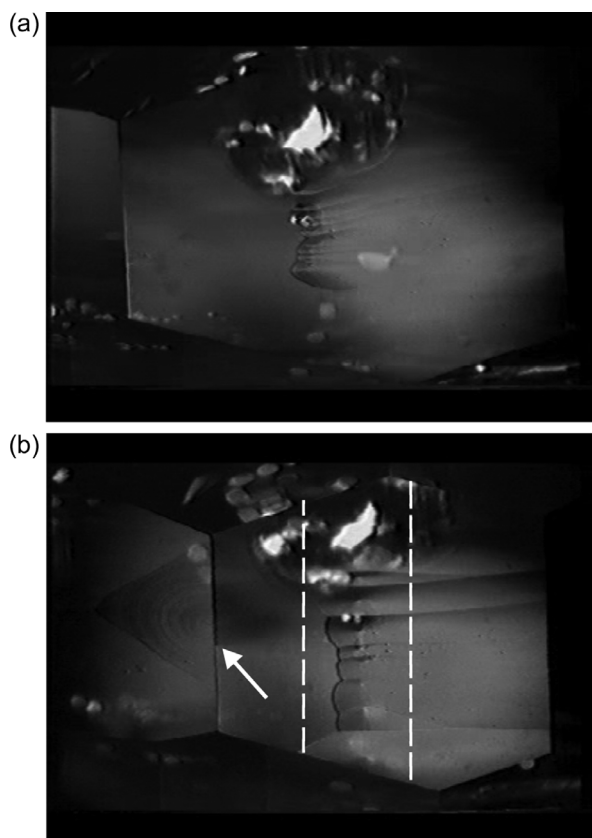


Figure 8. Continuation of video S4 after an interruption of the record of about 45 min. a) The growth hills of the dislocations arising from the inclusion start to form a vertical chain, indicating a fanning-out of these dislocations. This is more strikingly shown in (b). b) Here the row of hills is subject to a strong step flow from the left side, which originates from a source at the left crystal edge (arrow). This source also emits faint steps on neighbored left (101) face. The dashed lines indicate the cut of the slice for X-ray topography. (Video S5, Supporting Information).

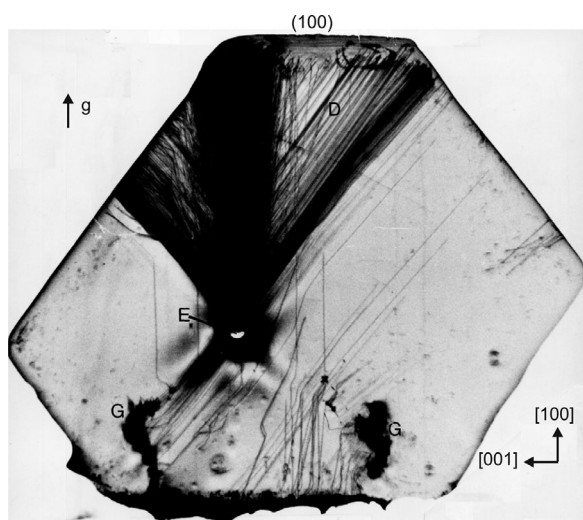


Figure 9. X-ray topograph of the (010) slice marked in Figure 8b, size $20 \times 17 \text{ mm}^2$, about 2 mm thick showing the fan of numerous dislocations arising from the ball inclusion, E. G: gas precipitates; g: diffraction vector (reflection 200); CuK α radiation.

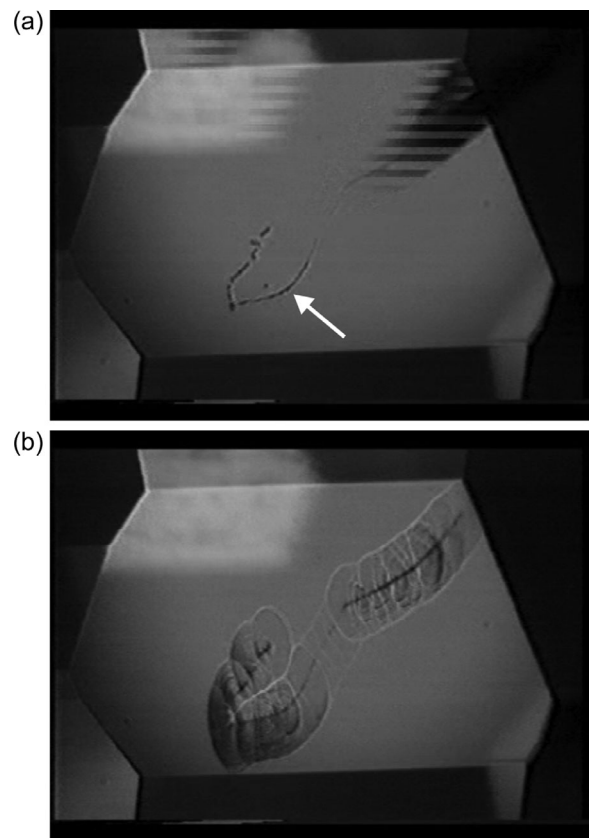


Figure 10. a) A (100) growth face (100) without any visible growth steps or growth hills in the moment of being scratched. b) Many growth hills develop along the scratch. (Video S6 Supporting Information).

dislocation-free or with only a few dislocations up to the inclusion, from which three bundles of dislocations originate, one normal to the (100) growth face, two parallel to the two lower [101] edges of the plate. Due to the relatively large size of the inclusions (0.5 mm), the number of generated dislocations and their density is partially so high that the dislocation lines could not be spatially resolved by X-ray topographic imaging.

Video S6, Supporting Information (Figure 10) shows the scratching of a seemingly perfect (100) face and the rapid development of growth hills. The topograph of a plate cut from another crystal subjected to a severe scratching experiment on the (100) face is given in Figure 11. Such severe impacts often trigger the precipitation of solute gas leading to bubbles and additional growth dislocations.

In this context we refer to a very subtle study of the generation of screw dislocations by inclusions in an organic crystal, growing from solution, on the sub-micrometer scale by in situ real-time atomic force microscopy (AFM).^[8] It reports that particles $<1 \mu\text{m}$ are frequently overgrown without dislocation creation, and it describes a case where two pairs of left- and right-handed screw dislocations are formed. In our present study, however, the particles are very large ($\approx 500 \mu\text{m}$). This implicates the mismatch of many layers overgrowing the inclusion and, consequently, the generation of many dislocations.

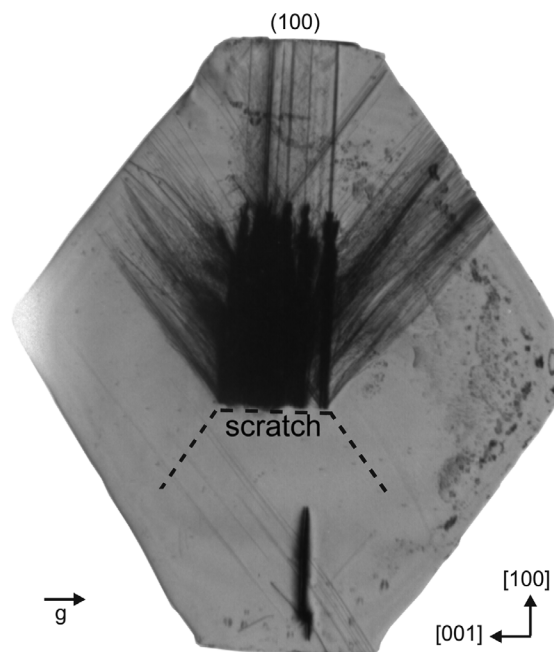


Figure 11. X-ray topograph of a (010) plate of salol ($20 \times 18 \text{ mm}^2$, 1 mm thick) showing traces of gas precipitates (black vertical columns) and numerous dislocations generated by a severe scratch on the (100) growth face. This scratch was done in direction [001] across the (100) facet at the respective stage of growth (indicated by the dotted lines) and is fully contained in the plate. The strong defect in the lower part is due to gas precipitation in an earlier stage of growth before scratching. g: diffraction vector (reflection 002), CuK α radiation.

Finally we quote two very detailed and comprehensive in situ atomic-force microscopy studies of the growth mechanisms and surface morphologies of zinc thiourea sulfate crystals.^[9,10] They present many sets of consecutive AFM records, which exhibit a plenty of instructive observations concerning 2D nucleation, the effect of edge and screw dislocations and the formation of pits in combination with the incorporation of microparticles.

4. Conclusion

Although the present study in principle does not provide new insights into the generation and propagation of dislocations, it shows many interesting features of their development and impacts upon the growth surface on which they emerge. Whereas former analogous experiments were performed on crystals growing from solutions or from the vapor phase, the present study concerns the growth of an organic crystal from supercooled melt under very simple and convenient conditions. Due to the high growth velocities long growth periods can be recorded within only a few hours or even minutes. The experiments show that immediately after the overgrowth of an inclusion a big

pyramid emitting fast growth steps is formed. They also show the interplay of different growth hills which mutually overgrow each other and re-appear. In the further course, the development of the dislocations originating from the inclusion in the shape of a fan is shown. Similarly, the fast formation of growth hills along a scratch on an originally flat face is recorded. X-ray topographs of slices properly cut from the final crystals and showing the dislocations generated by the inclusion and the scratch complete the study.

Supporting Information

Supporting Information is available from the Wiley Online Library or from the author.

Acknowledgements

The authors thank the *Stiftung Volkswagenwerk* for the support of this project (AZ. I/66711) and the Country *Nordrhein-Westfalen* for a scholarship (G.N.).

Conflict of Interest

The authors declare no conflict of interest.

Keywords

C₁₃H₁₀O₃, crystal growth, dislocations, inclusion formation, organic crystal, salol, supercooled melt, X-ray topography

Received: August 13, 2019

Revised: September 12, 2019

Published online: November 20, 2019

- [1] H. Klapper, in *Springer Handbook of Crystal Growth* (Eds: G. Dhanaraj, K. Byrappa, V. Prasad, M. Dudley), Springer, Berlin **2010**, pp. 93–132.
- [2] H. Klapper, P. Rudolph, in *Handbook of Crystal Growth*, 2nd ed., Vol. IIb (Eds: T. Nishinaga, P. Rudolph, T. Kuech), Elsevier, The Netherlands **2015**, pp. 1093–1141.
- [3] G. Neuroth, *Ph.D. Thesis*, University of Bonn **1996**.
- [4] G. Neuroth, H. Klapper, *Chem. Ing. Tech.* **1998**, *70*, 1535.
- [5] Th. Scheffen-Lauenroth, H. Klapper, R. A. Becker, *J. Cryst. Growth* **1981**, *55*, 557.
- [6] A. R. Lang, *Acta Crystallogr.* **1959**, *12*, 249.
- [7] H. Klapper, in *Crystals: Growth, Properties and Characterization*, Vol. 13 (Ed: N. Karl), Springer, Berlin **1991**, pp. 109–162.
- [8] X. Zhong, A. G. Shtukenberg, Th. Hueckel, B. Kahr, M. D. Ward, *Cryst. Growth Des.* **2018**, *18*, 318.
- [9] J. Song, M. Lie, M. Cheng, Z. Hu, Y. Cao, *Cryst. Res. Technol.* **2014**, *49*, 743.
- [10] J. Song, M. Lie, Y. Cao, H. Yin, *Cryst. Res. Technol.* **2015**, *50*, 828.